CONFERENCE PRE-PRINT

WEST WALL CONDITIONING WITH BORON: LESSONS FOR ITER AND FUSION POWER PLANTS

E. Geulin[1] (eleonore.geulin@cea.fr), A. Gallo[1], M. Diez[1], P. Manas[1], T. Wauters[2], J. Gaspar[3], E. Hodille[1], P. Puglia[1], N. Rivals[1], T. Alarcon[1], R. Bisson[4], E. Caprin[1], G. Ciraolo[1], Y. Corre[1], J. Denis[1], C. Desgranges[1], N. Fedorczak[1], P. Forestier-Colleoni[1], G. Gervasini[5], A. Grosjean[6], C. Guillemaut[1], B. Guillermin[1], J. Gunn[1], A. Hakola[7], J. Hobirk[8], K. Krieger[8], L. Laguardia[5], R. Lunsford[9], P. Maget[1], R. Mitteau[1], Ph. Moreau[1], R. Pitts[2], D. Sgrelli[1], E. Tsitrone[1], N. Varadara[1], S. Vartanian[1], A. Widdowson[10],
the WEST team[*], *EUROfusion WPTE team*[**]

[1] CEA, IRFM, Saint-Paul-les-Durance Cedex, France
[2] ITER Organization, 13067, Saint-Paul-Lez-Durance, France
[3] Aix-Marseille University, CNRS, IUSTI, Marseille, France
[4] Aix-Marseille University, CNRS, PIIM, F-13397, Marseille, France
[5] Istituto per la Scienza e Tecnologia dei Plasmi–CNR, Milano, Italy
[6] Department of Nuclear Engineering, University of Tennessee, USA
[7] VTT Technical Research Centre of Finland Ltd., PO Box 1000, 02044 VTT, Finland
[8] Max–Planck-Institut für Plasmaphysik, Boltzmannstr. 2, 85748, Garching, Germany
[9] PPPL, Princeton, NJ 08543, USA
[10] UKAEA, Culham Campus, Abingdon, OX14 3DB, UK

[*] WEST team: `http://west.cea.fr/WESTteam`
[**] See the author list of *Progress on an exhaust solution for a reactor using EUROfusion multimachines capabilities* by E. Joffrin *et al.*, Nuclear Fusion 2024

Abstract

Boronisation by glow discharge (GDB) is a key element of wall conditioning for devices with full-W walls. By depositing a thin, low-Z B layer that getters oxygen and mitigates tungsten source terms, GDB lowers radiative losses during breakdown and burn-through and widens the operational window for a reliable restart of plasma operations. WEST, equipped with actively cooled, ITER-grade tungsten plasma-facing components and long-pulse capability, provides a reactor-relevant environment to quantify these effects.
This study reports three main results. First, motivated by ITER constraints, a deliberately non-uniform GDB was implemented in WEST using all glow electrodes while injecting B_2D_6 from only half of the available toroidal locations; post-mortem analysis of samples exposed during this GDB via two toroidally separated sample holders with different expected B coverage showed a corresponding thickness asymmetry in the deposited B layer, yet sustained operation, including long pulses, remained feasible. Second, at restart after a vent, we contrasted limiter attempts without GDB with the same requests once GDB had been applied. The post-GDB cases met the specified pulse duration and plasma-current targets repeatedly, establishing the necessity of conditioning at restart. Third, pairs of nominally identical discharges executed immediately before and after GDB were used to characterise deuterium trapping: an early post-GDB rise in apparent retention was observed, followed by saturation with modest cumulative plasma time/energy, returning towards pre-GDB levels.
The results offer practical guidance for campaign preparation: GDB is required to ensure dependable restart, toroidally non-uniform deposition is tolerable for operation, and the immediate retention cost of fresh B layers relaxes after limited exposure—informing inventory control in ITER-relevant tungsten environments.

1. INTRODUCTION

Glow Discharge Boronisation (GDB) deposits a low-Z B layer across the whole vessel. By gettering oxygen across the vessel and briefly masking tungsten on plasma-facing components, GDB lowers Z_{eff} and early-phase radiation during breakdown and burn-through, widening the operating window [1, 2]. Accordingly, tokamaks routinely apply GDB to ease the restart of plasma operation, improving breakdown and current ramp-up and providing reliable access to routine and, where applicable, high-performance scenarios.
In ITER, GDB must contend with constraints unlike those of present devices: a larger vessel demands more boron to reach tens–hundreds of nm; long pulses and high fluence accelerate layer saturation and remobilisation; and limited port access constrains the number and toroidal placement of glow anodes and gas injection. During the Start of Research Operations, eight glow anodes are foreseen in ITER, but without toroidally symmetric coverage, making a toroidally non-uniform GDB layer a likely reality. Established modelling of the glow and of B_2D_6 dissociation predicts significant toroidal non-uniformities in diborane reaction rates within the glow volume [3, 4, 5].
Against this backdrop, we chose to test the operational consequences of a toroidally non-uniform GDB in WEST [6], a long-pulse tokamak (plasma up to 1337,s) with actively cooled tungsten plasma-facing components and an ITER-relevant tungsten monoblock divertor. WEST is equipped with six glow anodes and six toroidal B_2D_6 injection points; this versatile arrangement allowed us to reproduce an ITER-like non-uniform configuration. For this experiment, all six anodes were energised while only three of the six injection locations were used, to emulate a toroidally non-uniform GDB and assess whether the deposited boron layers are correspondingly non-uniform (Section 2). We then show that, following a vent, reliable restart of plasma operations is achieved after GDB even when implemented non-uniformly (Section 3). Finally, we quantify the immediate fuel-retention impact of GDB: an initial rise in deuterium retention that returns to pre-GDB levels once the B layers saturate (Section 4).

2. NON-UNIFORM GDB: RATIONALE, IMPLEMENTATION, AND TOROIDAL DEPOSITION

2.1. ITER-driven rationale and WEST implementation

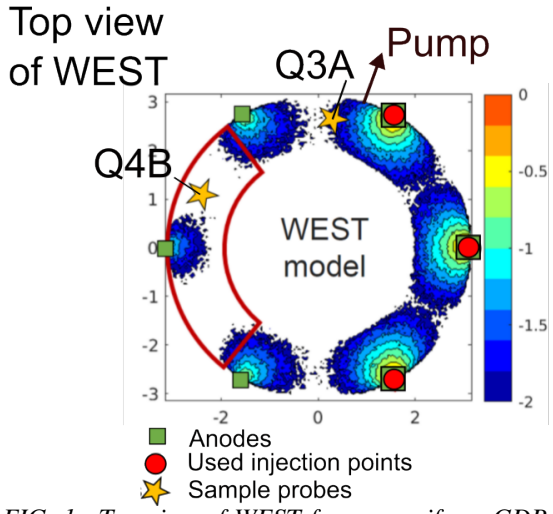

FIG. 1. Top view of WEST for non-uniform GDB: six glow anodes (green squares) and three B_2D_6 injectors located (red circles) on the equatorial plane. The colour map displays diborane dissociation and ionisation rates in a horizontal plane. The data are plotted on a logarithmic scale and normalised to the maximum reaction density. Predictions come from a 2D multi-fluid model with Monte Carlo tracing [3, 4, 5]. Sample holders: Q3A (near higher predicted reactivity) and Q4B (farther).

WEST is equipped with six glow anodes and six toroidal B_2D_6 injection points. For this experiment, all six anodes were energised while only three of the six injectors were used, to emulate a toroidally non-uniform GDB and assess whether the deposited B layers are correspondingly non-uniform. Figure 1 shows the anodes, injectors, and the expected toroidal pattern of B production from a 2D multi-fluid/Monte Carlo model [3, 4, 5]. Two toroidal sample holders were positioned accordingly: Q3A near a region of higher predicted reactivity and Q4B in a region of lower predicted reactivity, enabling a direct toroidal comparison under the same GDB.

2.2. Sample holders and qualitative findings

Two toroidal sample holders (locations in Fig. 1) were exposed during the same non-uniform GDB. Each holder has four faces (five samples per face) plus one underside sample ($4\times5+1 = 21$ positions); W and 316L samples were used. The photographs in Fig. 2 show the holders after GDB with the samples removed.

Post-mortem visual inspection indicates a toroidal thickness/morphology asymmetry. The Q4B sample "4E" appears bluish, whereas the Q3A sample "4A" shows a violet/pink tone. Both were immersed to the same depth in the glow and mounted on the same side of their holders (the side facing the outer wall), isolating toroidal location as the differentiating factor. On a given holder, samples at the same vertical position display similar colouration across faces, with differences mainly in intensity; the weakest apparent intensity is on the counter-clockwise face. Variations among the other faces are too subtle to resolve visually and will require quantitative post-mortem analysis. These qualitative differences (tint and intensity) are consistent with non-uniform GDB deposit. Quantitative post-mortem analyses (thickness, composition, density) are in progress.

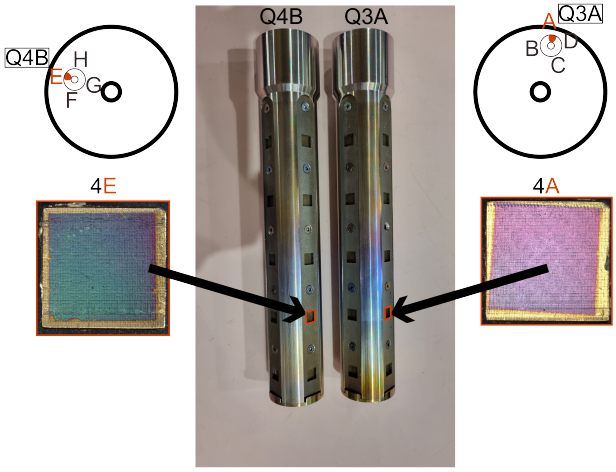

FIG. 2. Sample holders after non-uniform GDB: Q4B sample "4E" (bluish), both holders with stronger hues at Q3A, Q3A sample "4A" (violet/pink). Visual differences support toroidal non-uniformity.

3. RESTART OF PLASMA OPERATIONS IN A FULL-W ENVIRONMENT UNDER NON-UNIFORM GDB

A key ITER relevant question is whether a full W wall device can restart after a vent without GDB. To test this, WEST initially resumed operations post summer 2024 with no GDB. Each pulse had a single requested plasma current I_p; we began at I_p = 300 kA and, when this failed to produce stable plasmas, followed the standard practice of stepping I_p up on subsequent pulses. Success was defined solely as achieving a 10 s pulse.

The sequence comprised (i) repeated limiter pulses without GDB, (ii) application of the deliberately non-uniform GDB described above, and (iii) a repeat of the same requests. For visualisation, pulses are indexed by their position relative to GDB (negative: before; positive: after). Marker colour indicates the achieved I_p range for context only.

Before GDB (left of the divider), only a few pulses exceeded 1 s; many ended early because of radiative collapse despite modest pulse-to-pulse improvement [1, 2]. This behaviour persisted across the different requested I_p steps, indicating wall-driven limits on burn-through and early ramp-up.

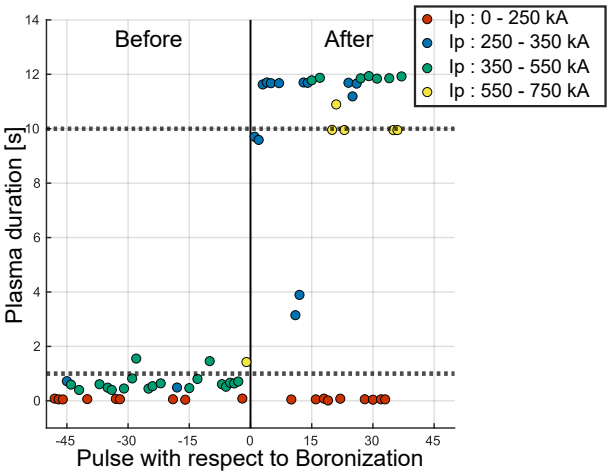

FIG. 3. Limiter restart attempts before/after non-uniform GDB. Abscissa: pulse index relative to GDB (negative: before; positive: after). Vertical black line: GDB. Marker colour encodes achieved I_p range.

Immediately after the non-uniform GDB (right of the divider), the same scenario requests produced plasmas lasting up to tens of seconds from the outset. In contrast, across four days and 75 restart trials without any GDB, only three pulses exceeded 1 s and none achieved the 10 s target. Early post GDB pulses were intentionally run at modest I_p (as per the planned stepping) while the wall conditioned; the requested 10 s duration was then met reproducibly, and the programme proceeded to higher I_p steps. The incidence of early terminations dropped sharply after GDB (9/37). Although there was some improvement before GDB, the best discharges still remained

below about 2 s, whereas immediately after GDB the pulses routinely exceeded 10 s. There is no evidence that similar reliability could have been achieved without GDB—and certainly not within an operationally acceptable timescale—so applying GDB at the start of a campaign is strongly recommended for a dependable restart in ITER relevant conditions.

4. IMPACT OF NON-UNIFORM GDB ON DEUTERIUM RETENTION

4.1. Experimental approach and retention metric

We analyse seven deuterium ohmic pulses with identical scenarios at $I_p = 400$ kA, but we do not use the first pulse of the day on either side of GDB. On the pre-GDB day, the very first pulse still reflects conditioning from the previous evening's glow, leading to an artificially elevated apparent retention; we therefore take the *second* pulse of that day as the pre-GDB reference. On the post-GDB day, the first pulse lacks complete pumping data in the afterglow, which would bias the retention estimate; we thus begin with the *second* pulse there as well. The dataset therefore consists of one pre-GDB reference (day-1, pulse #2) and six post-GDB pulses (day$+1$, pulses #2–#7). In both cases, the machine had just produced an identical ohmic pulse immediately beforehand, making the pre- and post-GDB groups directly comparable.

Integration window and definitions. All time integrals use a common window $[t_0, t_1]$ with $t_0 = -2.5$ s (before prefill onset) and t_1 the earliest end-time available across the seven pulses (so each pulse is integrated over the same duration, covering prefill, plasma, post-discharge recombination and afterglow, here is about ~ 35.4 s). Define

$$N_{\text{inj}} \equiv \int_{t_0}^{t_1} \dot{N}_{\text{inj}}(t)\, dt, \qquad \text{Pumped} \equiv \sum_{i \in \{midplane, divertor\}} \int_{t_0}^{t_1} S_i^{(\text{D}_2)}\, p_i(t)\, dt,$$

where $\dot{N}_{\text{inj}}(t)$ is the D_2 injection rate, $p_i(t)$ the chamber pressure at location i (converted to D_2 equivalent), and $S_i^{(\text{D}_2)}$ the effective D_2 pumping speed referred to the vessel. The net wall loading over the window is

$$N_{\text{load}} = N_{\text{inj}} - \text{Pumped},$$

and the retention fraction is

$$\text{Retention}\,[\%] = 100\, \frac{N_{\text{load}}}{N_{\text{inj}}}\,.$$

Throughout, D_2 is assumed to dominate the exhaust over $[t_0, t_1]$.

Uncertainty on N_{inj}. N_{inj} is estimated from three independent diagnostics: (i) a flowmeter at the injection outlet; (ii) a gauge on the buffer volume feeding injections; and (iii) two Baratron gauges upstream/downstream of that volume. Knowing the buffer volume, the pressure signals yield the gas quantity withdrawn over $[t_0, t_1]$. A weighted mean of the three estimates is taken; the standard deviation about this weighted mean defines $\sigma_{N_{\text{inj}}}$, with reduced weights for Baratron data near their lower range.

Uncertainty on Pumped (including pumping-speed calibration). All pressure gauges were calibrated on dedicated steady-pressure days against a chosen reference gauge (closest range to the Penning, most stable signal). For a given gauge,

$$p_{\text{gauge}} = (a \pm \sigma_a)\, p_{\text{ref}} + (b \pm \sigma_b),$$

with the reference plateau noise propagated into σ_a, σ_b. During pulses, the instantaneous uncertainty $\sigma_{p_i}(t)$ combines calibration terms and live noise.
In addition, the effective pumping speeds $S_i^{(\text{D}_2)}$ carry their own uncertainty, determined from off-plasma steady pressure plateaux with selected pumps enabled (e.g. midplane-only or divertor-only). On each plateau, mass balance gives $\Phi_{\text{pumped}} = \dot{N}_{\text{inj}}$, hence

$$S_i^{(\text{D}_2)} = \frac{\dot{N}_{\text{inj}}}{p_i}\,.$$

For a fixed pumping configuration we performed several plateaux, yielding $\{S_i^{(k)}\}_{k=1}^{K}$; we report

$$\bar{S}_i = \frac{1}{K} \sum_{k=1}^{K} S_i^{(k)}, \qquad \sigma_{S_i} = \sqrt{\frac{1}{K-1} \sum_{k=1}^{K} \big(S_i^{(k)} - \bar{S}_i\big)^2}.$$

By construction, σ_{S_i} is a statistical spread across plateaux (with each $S_i^{(k)}$ already corrected for its plateau-pressure uncertainty), so we treat σ_{S_i} as independent of the pulse-time pressure uncertainty $\sigma_{p_i}(t)$.
For the pumped throughput at station i,

$$\mathrm{Pumped}_i = \int_{t_0}^{t_1} \bar{S}_i \, p_i(t) \, dt,$$

the propagated variance is then

$$\sigma^2_{\mathrm{Pumped},i} = \Big(\bar{S}_i \int_{t_0}^{t_1} \sigma_{p_i}(t) \, dt \Big)^2 + \Big(\sigma_{S_i} \int_{t_0}^{t_1} p_i(t) \, dt \Big)^2,$$

with the cross term neglected due to independence. The total uncertainty combines stations in quadrature,

$$\sigma_{\mathrm{Pumped}} = \sqrt{\sum_i \sigma^2_{\mathrm{Pumped},i}} \, ,$$

and $\bar{S}_i$ is the value corresponding to the active pumping configuration during the pulses.

Summary. We thus compare seven like-for-like limiter pulses at $I_p = 400$ kA (one pre-GDB, six post-GDB), integrating all signals over a common $[t_0, t_1]$, and quoting error bars that combine (i) the weighted dispersion of three independent injection estimates and (ii) calibrated pressure uncertainties propagated through the pumping integral to obtain N_{load} and the retention fraction.

4.2. Results and operational implications

Figure 4(a) compares, for matched line-averaged core density, the time traces of the reference pre-GDB pulse (red) and the first post-GDB pulse used in the series (blue). Achieving a similar central density requires a larger injected D_2 quantity after GDB. The pumped throughputs (divertor and vessel) differ only at the level of their uncertainties, indicating no clear change in total exhaust within error bars.

Figure 4(b) shows the post-GDB retention fractions normalised to the retention of the reference pre-GDB pulse with the same scenario. Immediately after GDB the normalised retention exceeds unity, then decreases approximately exponentially and returns to a value comparable to the pre-GDB reference within about six ohmic pulses ($\sim$15 MJ cumulative plasma energy). We interpret this as saturation of the available deuterium trapping sites in the freshly deposited B layer. This does not imply that the impact of GDB vanishes thereafter; rather, its additional contribution to further D_2 uptake becomes small once the traps are filled, while other benefits persist—namely vessel-wide gettering on non–plasma-facing surfaces that keeps oxygen partial pressures, and thus edge radiation during breakdown/burn-through, low.

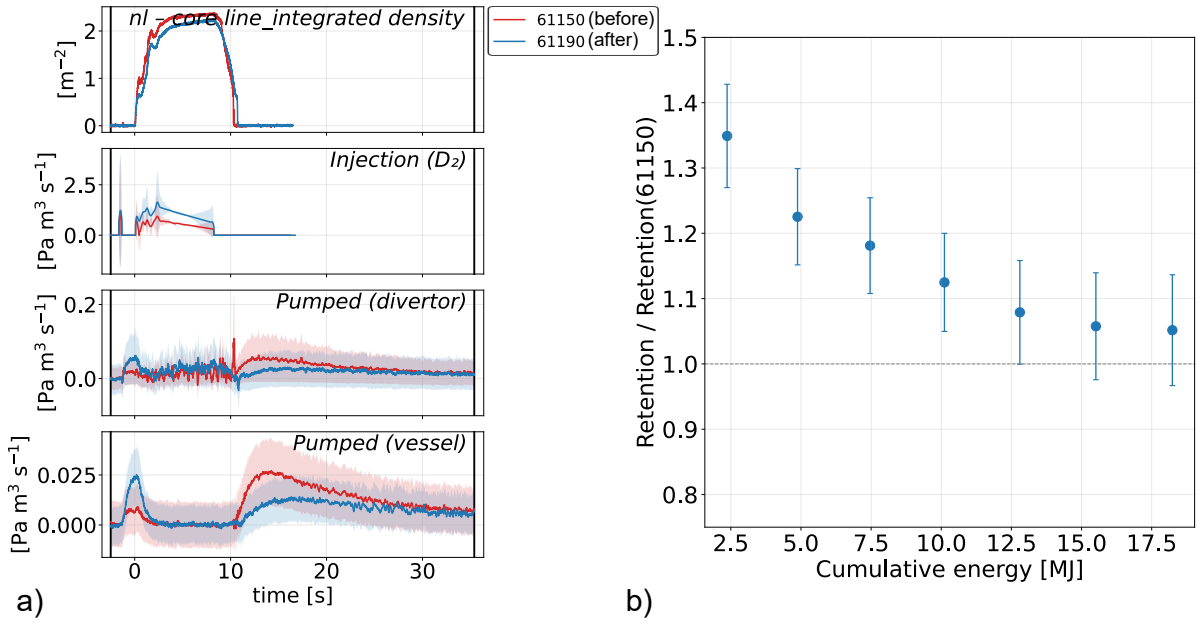

FIG. 4. (a) Time traces for the reference pre-GDB pulse (red) and the first post-GDB pulse used in the series (blue): from top to bottom, line-averaged core density (interferometer), injected D_2 quantity, and pumped throughput (divertor and vessel). (b) Normalised retention fraction for the post-GDB ohmic pulses, each point normalised to the pre-GDB reference (day−1, pulse #2) with identical scenario.

5. CONCLUSIONS

This work examined non-uniform glow discharge boronisation (GDB) in WEST. A deliberately toroidally non-uniform GDB produced clear toroidal differences in deposited B, as indicated qualitatively by sample holders placed at distinct locations. Despite the non-uniformity, a reliable restart after the vent was obtained only once GDB had been applied. Thereafter, deuterium wall retention rose initially but, after modest cumulative exposure, fell back towards pre-GDB levels, consistent with saturation of the fresh B layer. Importantly, the toroidally non-uniform GDB itself did not impose operational limits; WEST operated normally, and the subsequent GDB was not brought forward.

While these studies provide useful evidence on the operational consequences of non-uniform GDB in a full-W environment, important questions remain. In particular, a quantitative characterisation of the spatial non-uniformity (thickness, composition, density) and a clearer understanding of the mechanisms linking layer properties to changes in plasma performance and retention are still required. Future work will address these uncertainties to optimise wall conditioning strategies and improve tokamak operation.

ACKNOWLEDGEMENTS

This work has been carried out within the framework of the EUROfusion Consortium, funded by the European Union via the Euratom Research and Training Programme (Grant Agreement No 101052200 - EUROfusion). Views and opinions expressed are however those of the author(s) only and do not necessarily reflect those of the European Union or the European Commission. Neither the European Union nor the European Commission can be held responsible for them.

REFERENCES

REFERENCES

[1] J. Winter. “Wall conditioning of fusion devices by reactive plasmas”. In: *Journal of Nuclear Materials* 161.3 (1989), pp. 265–330. DOI: https://doi.org/10.1016/0022-3115(89)90466-2. URL: https://www.sciencedirect.com/science/article/pii/0022311589904662.

[2] A. Kallenbach et al. "Non-boronized compared with boronized operation of ASDEX Upgrade with full-tungsten plasma facing components". In: *Nuclear Fusion* 49.4 (2009), p. 045007. URL: https://iopscience.iop.org/article/10.1088/0029-5515/49/4/045007/meta.

[3] G. J. M. Hagelaar. "Modeling of glow discharges: from plasma chemistry to device design". In: *Plasma Physics and Controlled Fusion* 57 (2015), p. 025008. DOI: https://doi.org/10.1088/0741-3335/57/2/025008. URL: https://iopscience.iop.org/article/10.1088/0741-3335/57/2/025008.

[4] D. Kogut et al. "Modelling the ITER glow discharge plasma". In: *Journal of Nuclear Materials* 463 (2015), pp. 1113–1116. DOI: https://doi.org/10.1016/j.jnucmat.2014.10.078. URL: https://www.sciencedirect.com/science/article/pii/S0022311514007624.

[5] T. Wauters, G.J.M. Hagelaar, and R.A. Pitts. "Modeling input to the ITER glow discharge boronization system design". In: *Nuclear Materials and Energy* 42 (2025), p. 101891. ISSN: 2352-1791. DOI: https://doi.org/10.1016/j.nme.2025.101891. URL: https://www.sciencedirect.com/science/article/pii/S2352179125000316.

[6] A. Gallo et al. "Effect of spatially non-uniform boronization on plasma restart in WEST". In: *Plasma-Facing Materials and Components Conference (PFMC 2025) – Proceedings*. Conference presentation; results presented at PFMC 2025. 2025.